

Robust determination of optical path difference: fringe tracking at the IOTA interferometer

Ettore Pedretti, Wesley A. Traub, John D. Monnier, Rafael Millan–Gabet, Nathaniel P. Carleton, F. Peter Schloerb, Michael K. Brewer, Jean–Philippe Berger, Marc G. Lacasse and Sam Ragland.

epedretti@umich.edu

Ettore Pedretti, Wesley A. Traub, Sam Ragland, Nathaniel P. Carleton, Marc G. Lacasse are with the Smithsonian Astrophysical Observatory, 60 Garden Street, Cambridge, MA, 02138, USA. John Monnier and Ettore Pedretti are at the University of Michigan, Ann Arbor, MI 48109, USA. Rafael Millan–Gabet is at the Michelson Science Center, California Institute of Technology, Pasadena, CA 91125, USA. F. Peter Schloerb and Michael K. Brewer are with the University of Massachusetts, Amherst, MA 01003, USA. Jean–Philippe Berger is with the Laboratoire d’Astrophysique de Grenoble, BP 53 X, Grenoble Cedex 9, France.

We describe the fringe packet tracking system used to equalise the optical path lengths at the Infrared Optical Telescope Array (IOTA) interferometer. The measurement of closure phases requires obtaining fringes on three baselines simultaneously. This is accomplished using an algorithm based on double Fourier interferometry for obtaining the wavelength–dependent phase of the fringes and a group delay tracking algorithm for determining the position of the fringe packet. The comparison between data acquired with and without the fringe packet tracker shows about a factor 3 reduction of the error on the closure–phase measurement. The fringe packet tracker has been able so far to track fringes of signal–to–noise as low as 1.8 for stars as faint as $m_H = 7.0$. © 2018 Optical Society of America

OCIS codes: 120.0120, 120.2650, 120.3180.

1. Introduction

Observations performed with long–baseline ground–based optical/infrared interferometers are strongly affected by the turbulent atmosphere. Turbulence can reduce the visibility of

fringes in many ways as described by Porro et al¹ for pupil-plane (or coaxial) beam combination and Thureau² for image-plane beam combination. Turbulence randomly modulates the phases of the fringes which can then become unusable for image reconstruction. Using three or more telescopes removes the atmospheric phase contamination. This is done through the closure-phase technique pioneered in radio astronomy³ and only recently applied to long-baseline optical interferometry.⁴ The necessary condition for obtaining meaningful closure-phases is that the three fringe packets must be detected within the coherence time. This is achieved by keeping the optical path difference (OPD) to a minimum.

Prior to 2002, IOTA had only two telescopes and a single baseline, and the fringes were usually kept inside the scan interval manually by the observers. The installation of the third telescope at IOTA required an increase in the level of automation in the instrument, because manual tracking is not practical with three baselines to adjust. In particular the requirement to measure closure-phases necessitated a system capable of keeping the fringe packets in the centre of the scan using the existing hardware dedicated to acquiring data. Fringes must be acquired in the same coherence time in order to measure a closure-phase. This is especially important at IOTA where the bandwidths are frequently relatively large (15–25%) and the fringe packets quite narrow (3–6 fringes).

We present here a simple and fast algorithm, which uses double Fourier interferometry (DFI)⁶ to extract wavelength dependent information from the fringe packet and calculate its group delay. The same algorithm was independently discovered by Tubbs⁵ and written as a final-year undergraduate project but never published. In this report Tubbs tested the algorithm through simulated data and data obtained from the COAST interferometer, but did not implement a working fringe-packet tracker. We only became aware of this work after our algorithm was routinely used at the IOTA.

The time-domain interferograms, recorded by an infrared detector for the purpose of measuring the physical parameters of stellar objects, are used in order to track the position of fringes. A fringe packet is generated by pupil-plane interference of starlight from two telescopes, where the optical path difference around the zero-path-difference point is changed linearly with time. Each pair of the three telescopes generates two such interferograms, with complementary intensities. The goal is to control the optical paths such that these interferograms occur nearly simultaneously, so that the closure phase can be measured from them. To do this, the algorithm in the present paper is applied to each fringe packet, and the output of the algorithm is used to control the optical paths before the next interferogram is produced. Up to about 10 interferograms are generated per second, using triangular sweeps of the optical paths. No additional hardware is required.

The application of the algorithm is not restricted to stellar interferometry but can be applied to all cases where broad-band interference fringes must be tracked. Other algorithms

for fringe packet tracking which have been tested at IOTA are the subjects of separate publications.⁷⁻¹¹

2. The Instrument

IOTA is a long-baseline optical interferometer located at the Smithsonian Institution's Whipple Observatory on Mount Hopkins, AZ, comprising three 45-cm diameter telescopes which can be positioned at 17 stations on an L-shaped track, where the arms are 15 m toward the south-east and 35 m toward the north-east. IOTA operated with 2 telescopes from 1995-2003, and 3 telescopes since February 2002. The interferometer,^{12,13} has been used as a testbed for new cutting-edge technologies,¹⁴⁻¹⁶ and has produced astronomy results in the 3-telescope configuration.¹⁷⁻²¹

The three beams arriving from the vacuum delay-line tank hit three dichroic mirrors which separate the visible and infrared light. The visible beam continues toward the star tracker servo system. In the implementation discussed here, the infrared beam is reflected toward three flat mirrors and then three off-axis parabolas which focus the three beams on three single-mode (H-band) fibers feeding the IONIC-3T integrated-optics beam-combiner.²²

Interference is achieved inside the integrated optics component, resulting in three output pairs π radians out of phase in intensity. The interference fringes are recorded while two of the dichroics are piezo-driven to scan a path of about $+50 \mu\text{m}$ and $-50 \mu\text{m}$, respectively, in order to scan through the fringe packet in the three beams. The six combined beams are then focused on six separate pixels of the PICNIC array¹⁶ and recorded as time series for science measurement. The same time series is used by the fringe-packet tracker. The path difference calculated by the packet-tracker is fed back to the piezo-scanning dichroics for a fast tracking response. The piezo scanners are off-loaded of their additional offsets every second, when a fraction of the error signal is sent to the short delay lines which are responsible for tracking the geometric delay caused by the rotation of the Earth.

3. Calculating the Fringe Position

3.A. Tracking the Fringe Packet Using Double Fourier Interferometry

Our method of fringe packet tracking at IOTA calculates the group delay of fringes dispersed with DFI, which is used to obtain the wavelength dependent phase from the fringe packet. This is done by scanning the fringe packet over an interval greater than the packet length, where the spectral resolution is proportional to the scan length. The group delay tracking (GDT) method has been applied to interferometry since the very beginning of the field, when Michelson²³ used a prism for dispersing and acquiring fringes visually at the 20-ft interferometer. Labeyrie²⁴ used the same system and demonstrated fringe acquisition on a two-telescope interferometer.

Several systems have been proposed since then, for correcting the optical path.^{25,26} GDT (also called dispersed fringe tracking when applied to image plane interferometry) has been routinely used at several interferometric facilities.^{27–29} In fact, at IOTA, GDT was selected as the original method of path difference monitoring in the visible,^{30–33} but the system was set aside in favor of making infrared observations.

We will perform now a derivation of the algorithm for a two-telescope interferometer which combines the light in the pupil plane through a beam-splitter. With this setup the light intensity $I(\xi)$ from the two complementary outputs of the beam-splitter is measured by square-law detectors:

$$I(\xi) = I_t \left\{ 1 \pm V \frac{\sin [\pi (\xi - \xi_0) \Delta f]}{\pi (\xi - \xi_0) \Delta f} \sin [2\pi (\xi - \xi_0) f_0 + \phi] \right\}, \quad (1)$$

where I_t is the mean intensity which becomes split by the beam combiner (\pm is for complementary outputs) and is modulated by the interferometric signal, function of the optical path ξ . V is the contrast of the fringes, Δf (cm^{-1}) the bandwidth of the ideal (rectangular) spectral filter, f_0 (cm^{-1}) the frequency of the fringe, ϕ (rad) a generic phase, and ξ_0 (cm) is the fringe-packet centre, which varies from scan to scan owing to atmospheric path fluctuation. This is the actual value we want to calculate in order to correct the optical path.

In practice we are dealing with discrete intensities, expressed as a finite series of data, so we can rewrite (1) as the discrete function $n(j)$, which is the detector count.

$$n(j) = n_0 \left\{ 1 \pm V \frac{\sin [\pi (j - J_0) \Delta m]}{\pi (j - J_0) \Delta m} \sin [2\pi (j - J_0) m_0 + \phi] \right\} + \epsilon_j \quad (2)$$

Here n_0 is the mean number of electrons per channel, and V is the fringe visibility. The sample number j ranges from 1 to N , where N is the total number of samples; typically $N = 256$. The centre of the fringe packet is at sample number J_0 . If the high- and low-wavenumber limits of the spectral filter are written as m_h and m_l (waves per sample), then the filter full-width at half-maximum is $\Delta m = m_h - m_l$, and the filter centre is $m_0 = (m_h + m_l)/2$, both in units of waves (or fringes) per sample. The phase ϕ (radians) is an offset between the sinusoid carrier wave and the centre of the sinc envelope. The ϵ_j term represents additive noise, the sum of electron counting statistics, detector read noise, and random atmospheric scintillation. The goal is to extract an estimate of J_0 from the ensemble of N data points.

The first step is to calculate the fast Fourier transform of the data string $n(j)$, and scaling the result so as to eliminate uninteresting factors. The result is a sequence of $N/2$ complex numbers which can be written as

$$\tilde{n}(m_0) = \exp(-i2\pi m_0 J_0) + \eta_{m_0} \quad (3)$$

where η_{m_0} is the scaled transform of the noise term ϵ_j .

The second step is to select two of the \tilde{n} values, say $\tilde{n}(m_0)$ and $\tilde{n}(m_0 + \Delta m_{12})$, and form the cross-spectrum product of the first with the complex conjugate of the second, i.e.,

$$X(m_0, m_0 + \Delta m_{12}) = \tilde{n}(m_0) \cdot \tilde{n}(m_0 + \Delta m_{12})^* . \quad (4)$$

As can be seen from (3), the cross-spectrum X will generate a complex number (plus noise) whose phase contains the unknown quantity J_0 , multiplied by known terms. The additive noise would degrade our estimate of J_0 from the cross spectrum term, however adding several such terms will improve the signal-to-noise ratio of the resulting complex term,³⁴ and likewise improve our estimate of J_0 .

The third step is to calculate the average cross-spectrum \overline{X} , as for example in

$$\overline{X} = \sum_{m_0=m_l}^{m_h} \frac{X(m_0, m_0 + \Delta m_{12})}{(m_h - m_l + 1)} = \exp(-i2\pi\Delta m_{12}J_0) + \overline{\eta}, \quad (5)$$

where $\overline{\eta}$ is the new noise term, presumably smaller than the root-mean-square of η_{m_0} by a factor on the order of $\sqrt{(m_h - m_l + 1)}$. The limits on the sum are only suggested values, and could be changed so as to improve the signal-to-noise ratio if applicable.

(We note that the cross-spectrum is also used in the Knox-Thompson algorithm³⁵ for recovering near diffraction-limited images of stellar objects from snapshots degraded by atmospheric seeing.)

The estimated fringe packet position $\langle J_0 \rangle$ can now be recovered from the average cross-spectrum using

$$\langle J_0 \rangle = \frac{\arg(\overline{X})}{2\pi\Delta m_{12}} . \quad (6)$$

Here the estimated packet center $\langle J_0 \rangle$ is measured in units of sample numbers from the first point in the interferogram. In practice we subtract $N/2$ from this value, and send the resulting value (suitably scaled) as an error signal to the servo system, such that the starting point of the next scan is adjusted accordingly.

We note that any value of Δm_{12} could be used, but we suggest that $\Delta m_{12} = 1$ is optimum in the sense that it is least likely to produce a complex S or \overline{S} that is biased by wrap-around effects, which will occur if the phase shift between adjacent values of \tilde{n} are separated by more than π . Hereafter we drop the expectation value brackets, and write J_0 for $\langle J_0 \rangle$ for notational simplicity.

3.B. Algorithm summary

1. The interference fringes are recorded while two of the optical paths are piezo-driven to scan a path of about $+50 \mu\text{m}$ and $-50 \mu\text{m}$, respectively. The time series n_j is recorded by the infrared camera for the three pairs of beams.

2. The fast Fourier transform $\tilde{n}(m_0)$ of the time series n_j is computed separately for the three pairs.
3. The cross-spectrum X is calculated for the 3 beams by multiplying $\tilde{n}(m_0)$ by its complex conjugated $\tilde{n}^*(m_0 + 1)$ shifted by one sample.
4. The average cross-spectrum \overline{X} is computed in correspondence of the fringe peak in the cross-power-spectrum, in order to average complex vector with higher signal-to-noise.
5. The position of the fringe packets is obtained from the phase of the average vector \overline{X} . using Eqn. 6

3.C. Baseline Bootstrapping

With baseline bootstrapping^{36,37} we are capable of blind-tracking fringes on a baseline when the signal-to-noise of the fringes is too low, provided that good signal-to-noise is available on the other two baselines. For this reason, we calculate the optical path J_0 for three baselines even if we correct the path for two baselines. We can express one optical path as the weighted average of the other two optical paths, the weights being equal to the SNR for the fringes obtained on those baselines. The signal-to-noise is calculated from the cross spectrum $|X|^2$, dividing the averaged power inside the fringe peak by the averaged power outside the fringe peak. We then observe that the optical path, in a closed loop must be equal to zero:

$$J_01 + J_02 + J_03 = 0 \quad (7)$$

where J_01 and J_02 are the optical path where the servo loop is acting, while J_03 is the reference optical path. To the path J_01 , J_02 and J_03 are associated the weights $w1$, $w2$ and $w3$ respectively. We have two values for each optical path. One is the value obtained directly on that baseline (for example J_01 with weight $w1$), the other is the value calculated from the linear combination of the other two baselines (for example $J_01' = -J_02 - J_03$ with weight $w1' = (w2w3)/(w2 + w3)$). The weighted average of J_0 and J_0' can then be written as:³⁸

$$\overline{J_01} = \frac{w1J_01 + w1'J_01'}{w1 + w1'} \quad (8)$$

where $\overline{J_01}$ is the weighted-averaged path difference. Similarly for $\overline{J_02}$:

$$\begin{aligned} \overline{J_02} &= \frac{w2J_02 + w2'J_02'}{w2 + w2'} \\ J_02' &= -J_01 - J_03 \\ w2' &= \frac{w1w3}{w1 + w3} \end{aligned} \quad (9)$$

The advantage of using a weighting system is that we do not have to select the best baseline values a priori, but rather the weighting allows them to be selected automatically.

4. Simulations

The linearity of the fringe packet tracker (FPT) algorithm was tested through simulations. This simulation was performed in presence of photon and detector noise, with an average number of 300 photoelectron/sample for the fringe intensity (Poisson distributed), a fringe visibility of one and an additional 12-electron mean of Gaussian noise for the detector.

It was found that the algorithm is capable of detecting the sign of the correction, necessary to bring back the fringes to the centre of the scan even if the main part of the fringe packet is outside the current scan. The necessary condition is to have enough signal-to noise so that the side lobes are detectable. This behavior is shown in the graph of Fig. 1.

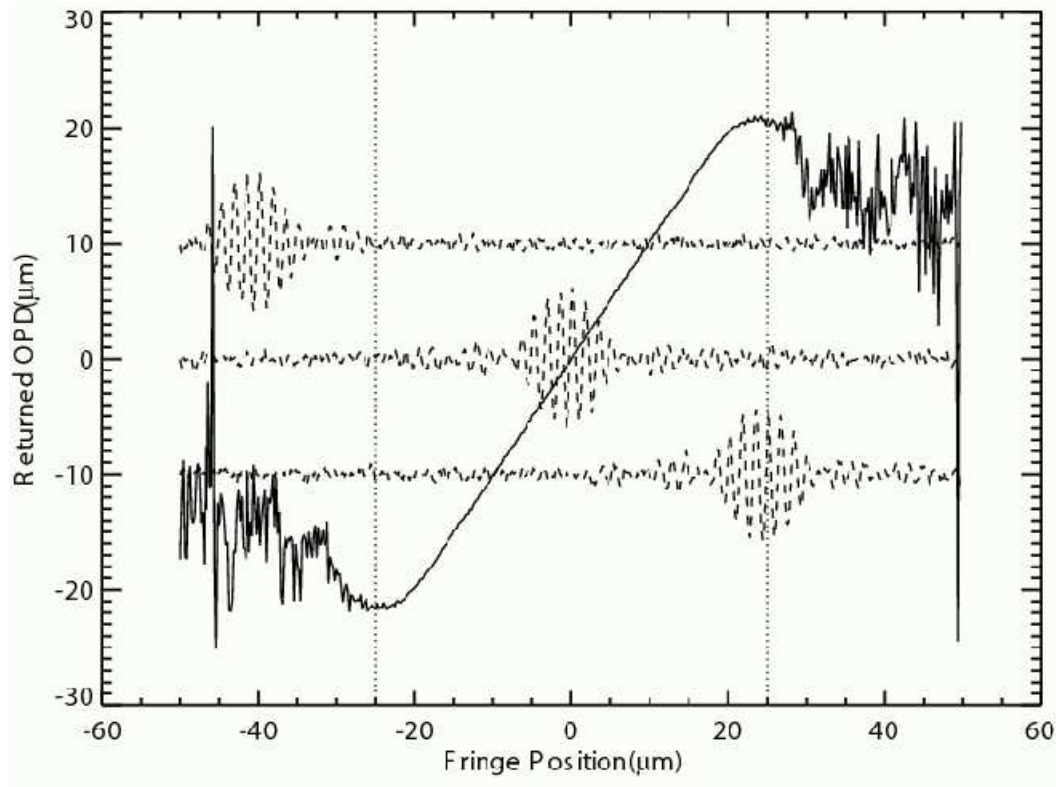


Fig. 1. The optical path returned by the algorithm with respect to the fringe position (continuous-line plot). The two vertical dotted-lines represent the interval inside of which the fringes are sampled, for a scan length of $50 \mu m$. Three fringe packets (dashed-lines) mark three representative positions on the plot: outside the scan range (top), at the centre of the scan (centre) and half outside the scan range (bottom). Note that only the side lobes are visible in the scan range of the plot at the top.

The returned position depends linearly on the fringe positions when the packet is inside the scan but it is non-linear when the packet is outside the scan. Nevertheless the information of the side lobes can still be used to bring the fringes back to the centre of the scan. The algorithm is sensitive to the slope of the phase across the bandwidth and the sign of the correction is preserved. The algorithm starts to fail at the limit of the range where the signal is too low and the side lobes not detectable for the given integration time. The returned position depends linearly on the fringe positions when the packet is inside the scan and becomes strongly non-linear (but with the correct sign) when the packet is outside the scan.

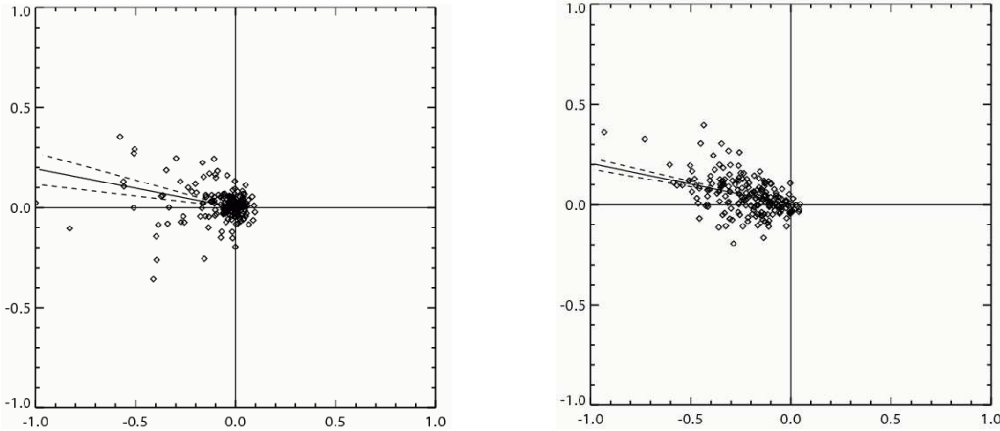


Fig. 2. Closure phase measurement for the star WR140 ($m_H = 5.3$). The points represented on the plot are complex vectors normalised by the signal-to-noise. Each point is calculated using a single fringe measurement for each baseline (notably the N-S, N-W and W-S baselines, where the telescopes were positioned at N=35m, S=15m and W=10m). There are 200 points in the diagram. The vector represented in solid line is the average closure phase of the previous 200 vectors and the dashed line represents the error on the closure phase. Finally the left panel represents a closure phase measurement in open-loop mode (FPT not active, closure phase = 169.0 ± 4.3 deg) while the right panel is the closed-loop case (FPT active, closure phase = 168.4 ± 1.5 deg).

5. Results

The FPT has been routinely in use at the IOTA interferometer since early 2002. Fig. 3 shows the reduction of tracking residuals operated by the algorithm. A reduction of about a factor 2 in the RMS change of the optical path, between data acquired with tracking switched off

compared to data with tracking on, can be shown from the recorded data. This lies mostly in the low frequency zone because of the limited bandwidth of the combined fringe-sensor, fringe-actuator. For the IOTA interferometer this is a significant improvement, since the high frequency phase noise is dealt within post-processing using the closure-phase information.

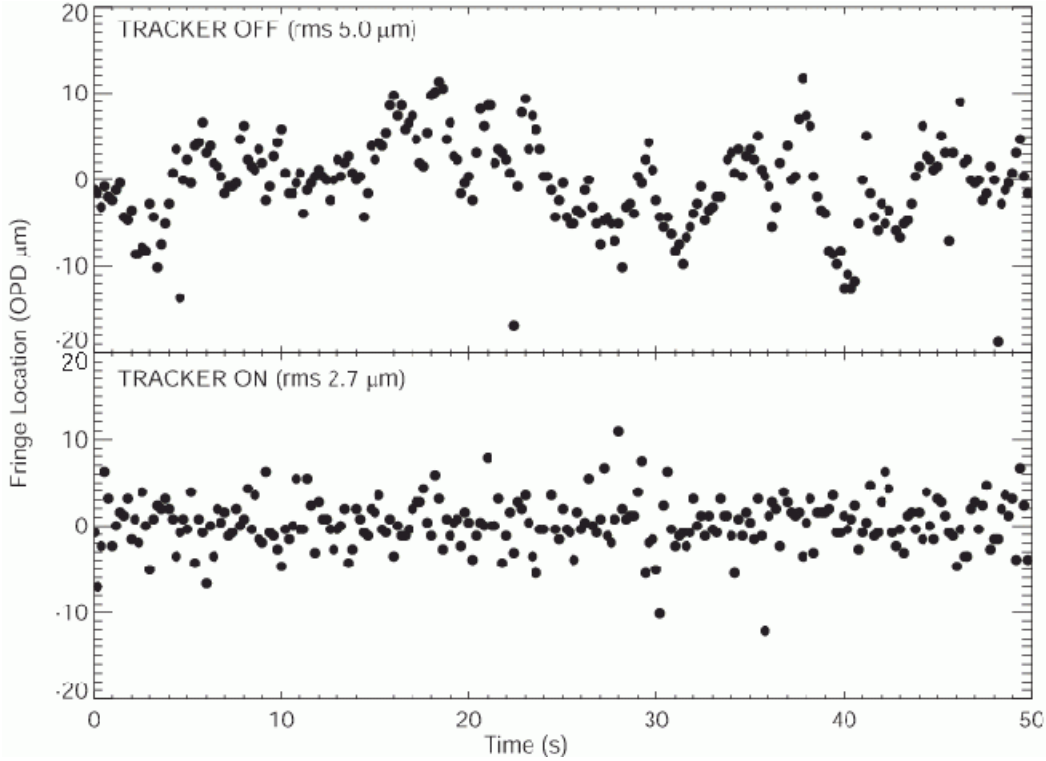


Fig. 3. The change of the OPD with the FPT turned off (top) and on (bottom). This experiment was performed using a single, 21 m long baseline at $1.65 \mu\text{m}$, during average seeing and no baseline bootstrapping. The data was recorded the 6th of March 2002. We measure a factor 2 reduction in the RMS change in optical path.

It is in fact more important to be able to maintain the fringe packet superposed and being able to do so for faint sources rather than reduce the residuals of the OPD to a smaller value. Fig. 2 shows two measurements of closure phase. When the FPT is switched off the closure phase is 169.0 ± 4.3 deg but it is 168.4 ± 1.5 deg when the FPT is operating (a factor 3 error reduction for the closed-loop case).

We also show that the FPT is capable to track fringes on a $7.0 m_H$ star with a SNR as low as 1.8 as shown in Fig. 4.

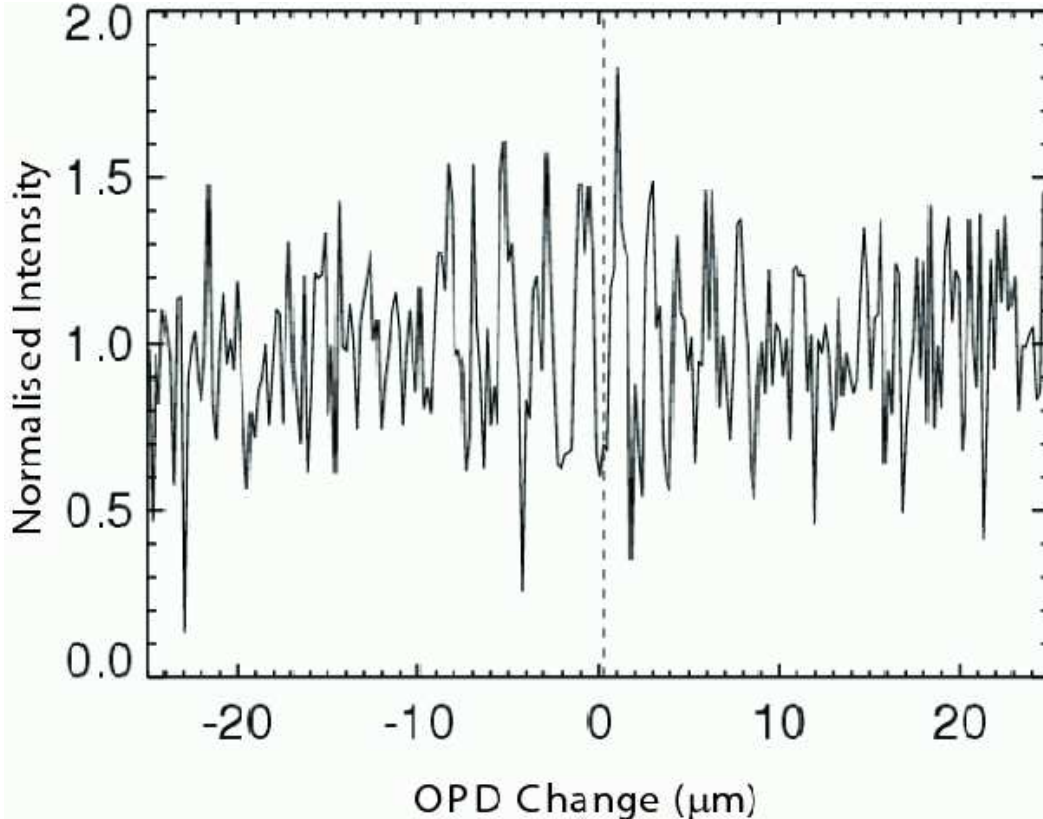


Fig. 4. Faint fringe observed on a $7.0 m_H$ star, yielding a SNR of 1.8. The dashed line across the fringe shows the expected position calculated by the FTP.

6. Conclusions

We describe the fringe packet tracking system now routinely in use at the IOTA interferometer. The packet tracker uses existing hardware to perform its functions, notably the infrared camera used for data acquisition, as a fringe sensor and the fringe scanning platforms combined with the delay lines, for correcting the optical path. It is based on an algorithm which exploits the wavelength-dependent information contained in the fringe packet, which is extracted using double Fourier interferometry. The phase of the fringes obtained for different frequencies is used for calculating the group delay of the fringe packet. Since we use baseline bootstrapping we are capable of blind-tracking fringes on a baseline when their signal-to-noise is very low, provided that the fringes have a good signal-to-noise on the other two baselines of the interferometer.

We use numerical simulation to model the case of a fringe packet outside the scanning range, operated by the algorithm, when only the side lobes of the fringe packet are visible.

We also show that the fringe packet tracker algorithm effectively reduces the slowly varying atmospheric and instrumental-induced additional path, leaving the fast phase noise to be dealt with post-processing. Moreover the FPT delivers about a factor 3 reduction of the error on the closure-phase measurement and has been able so far to track fringes with SNR as low as 1.8.

7. Acknowledgments

This research was made possible thanks to a Smithsonian Predoctoral Fellowship and a Michelson Postdoctoral Fellowship awarded to E. Pedretti. The IONIC project is a collaboration among the Laboratoire d’Astrophysique de Grenoble (LAOG), Laboratoire d’Electromagnetisme Microondes et Optoelectronique (LEMO), and also CEA-LETI and IMEP, Grenoble, France. The IONIC project is funded in France by the Centre National de Recherche Scientifique and Centre National d’Etudes Spatiales. The work and the fringe packet tracker were supported in part by grant NAG5-4900 from NASA, by grants AST-0138303 from the NSF, and by funds from the Smithsonian Institution. This research has made use of NASA’s Astrophysics Data System Bibliographic Services.

References

1. I. L. Porro, W. A. Traub, and N. P. Carleton, “Effect of Telescope Alignment on a Stellar Interferometer,” *Appl. Opt.***38**, 6055–6067 (1999).
2. N. D. Thureau, “Contribution à l’interférométrie optique à longue base en mode multi-tavelures,” Ph.D. thesis, Université de Nice-Sophia Antipolis - Faculté des sciences (2001).
3. R. C. Jennison, “A phase sensitive interferometer technique for the measurement of the Fourier transforms of spatial brightness distributions of small angular extent,” *MNRAS***118**, 276–284 (1958).
4. J. E. Baldwin, M. G. Beckett, R. C. Boysen, D. Burns, D. F. Buscher, G. C. Cox, C. A. Haniff, C. D. Mackay, N. S. Nightingale, J. Rogers, P. A. G. Scheuer, T. R. Scott, P. G. Tuthill, P. J. Warner, D. M. A. Wilson, and R. W. Wilson, “The first images from an optical aperture synthesis array: mapping of Capella with COAST at two epochs.” *A&A***306**, L13–L16 (1996).
5. R. N. Tubbs, “Tracking and Characterising Atmospheric Phase Fluctuations at COAST,” Part III undergraduate project report, May 1998, Cavendish Laboratory, Cambridge University (1998). URL http://www.geocities.com/CapeCanaveral/2309/phase_track.html.

6. J.-M. Mariotti and S. T. Ridgway, “Double Fourier spatio-spectral interferometry - Combining high spectral and high spatial resolution in the near infrared,” *A&AS* **195**, 350–363 (1988).
7. E. Wilson and R. W. Mah, “Online fringe tracking and prediction at IOTA,” in *Proc. SPIE Vol. 3749, 18th Congress of the International Commission for Optics, Alexander J. Glass; Joseph W. Goodman; Milton Chang; Arthur H. Guenther; Toshimitsu Asakura; Eds.*, pp. 691–692 (1999).
8. S. Morel, W. A. Traub, J. D. Bregman, R. W. Mah, and E. Wilson, “Fringe-tracking experiments at the IOTA interferometer,” in *Proc. SPIE Vol. 4006, Interferometry in Optical Astronomy, Pierre J. Lena; Andreas Quirrenbach; Eds.*, pp. 506–513 (2000).
9. N. D. Thureau, R. C. Boysen, D. F. Buscher, C. A. Haniff, E. Pedretti, P. J. Warner, and J. S. Young, “Fringe envelope tracking at COAST,” in *Interferometry for Optical Astronomy II. Edited by Wesley A. Traub . Proceedings of the SPIE, Volume 4838, pp. 956-963 (2003).*, pp. 956–963 (2003).
10. E. Wilson, E. Pedretti, J. D. Bregman, R. Mah, and W. A. Traub, “Adaptive DFT-based interferometer fringe tracking,” to appear in *EURASIP Journal on Applied Signal Processing* (2005).
11. E. Wilson, E. Pedretti, J. D. Bregman, R. Mah, and W. A. Traub, “Adaptive DFT-based fringe tracking and prediction at IOTA,” in *Proc. SPIE, New Frontiers in Stellar Interferometry, Wesley A. Traub; Ed.*, vol. 5491 (2004).
12. W. A. Traub, N. P. Carleton, J. D. Bregman, M. K. Brewer, M. G. Lacasse, P. Maymoukov, R. Millan-Gabet, J. D. Monnier, S. Morel, C. D. Papaliolios, M. R. Pearlman, I. L. Porro, F. P. Schloerb, and K. Souccar, “Third telescope project at the IOTA interferometer,” in *Proc. SPIE, Interferometry in Optical Astronomy, Pierre J. Lena; Andreas Quirrenbach; Eds.*, vol. 4006, pp. 715–722 (2000).
13. W. A. Traub, A. Ahearn, N. P. Carleton, J. Berger, M. K. Brewer, K. Hofmann, P. Y. Kern, M. G. Lacasse, F. Malbet, R. Millan-Gabet, J. D. Monnier, K. Ohnaka, E. Pedretti, S. Ragland, F. P. Schloerb, K. Souccar, and G. Weigelt, “New Beam-Combination Techniques at IOTA,” in *Interferometry for Optical Astronomy II. Edited by Wesley A. Traub. Proceedings of the SPIE, Volume 4838, pp. 45-52 (2003).*, pp. 45–52 (2003).
14. J. P. Berger, P. Haguenaue, P. Kern, K. Perraut, F. Malbet, I. Schanen, M. Severi, R. Millan-Gabet, and W. Traub, “Integrated optics for astronomical interferometry. IV. First measurements of stars,” *A&A* **376**, L31–L34 (2001).
15. J. D. Monnier, J. P. Berger, R. Millan-Gabet, W. A. Traub, N. P. Carleton, E. Pedretti, C. M. Coldwell, and C. D. Papaliolios, “SMART Precision Interferometry at 794 nm,” in *Proc. SPIE, Interferometry for Optical Astronomy, Wesley A. Traub, editor*, vol. 4838, pp. 1127–1138 (2003).

16. E. Pedretti, R. Millan-Gabet, J. D. Monnier, W. A. Traub, N. P. Carleton, J.-P. Berger, M. G. Lacasse, F. P. Schloerb, and M. K. Brewer, “The PICNIC Interferometry Camera at IOTA,” *PASP***116**, 377–389 (2004).
17. J. D. Monnier, R. Millan-Gabet, P. G. Tuthill, W. A. Traub, N. P. Carleton, V. Coude du Foresto, W. C. Danchi, M. G. Lacasse, S. Morel, G. Perrin, and I. Porro, “Aperture synthesis using multiple facilities: Keck aperture masking and the IOTA interferometer,” in *Proc. SPIE, Interferometry for Optical Astronomy*, Wesley A. Traub, editor, vol. 4838, pp. 379–386 (2003).
18. K. Ohnaka, U. Beckman, J. P. Berger, M. K. Brewer, K. Hofmann, M. G. Lacasse, V. Malanushenko, R. Millan-Gabet, E. Pedretti, J. D. Monnier, D. Schertl, F. P. Schloerb, V. Shenavrin, and W. A. Traub, “IOTA observation of the circumstellar envelope of R CrB,” in *Proc. SPIE, Interferometry for Optical Astronomy*, Wesley A. Traub, editor, vol. 4838, pp. 1068–1071 (2003).
19. R. Millan-Gabet, E. Pedretti, J. D. Monnier, W. A. Traub, F. P. Schloerb, N. P. Carleton, S. Ragland, M. G. Lacasse, W. C. Danchi, P. Tuthill, G. Perrin, and V. Coudé du Foresto, “Recent Science Results from the Two-Telescope IOTA,” in *Proc. SPIE, Interferometry for Optical Astronomy*, Wesley A. Traub, editor, vol. 4838, pp. 202–209 (2003).
20. G. Weigelt, U. Beckman, J. P. Berger, T. Bloecker, M. K. Brewer, K. Hofmann, M. G. Lacasse, V. Malanushenko, R. Millan-Gabet, J. D. Monnier, K. Ohnaka, E. Pedretti, D. Schertl, F. p. Schloerb, M. Scholz, W. A. Traub, and B. Yudin, “JHK-band spectrophotometry of T Cep with the IOTA interferometer,” in *Proc. SPIE, Interferometry for Optical Astronomy*, Wesley A. Traub, editor, vol. 4838, pp. 181–184 (2003).
21. J. D. Monnier, W. A. Traub, F. P. Schloerb, R. Millan-Gabet, J.-P. Berger, E. Pedretti, N. P. Carleton, S. Kraus, M. G. Lacasse, M. Brewer, S. Ragland, A. Ahearn, C. Coldwell, P. Haguenaue, P. Kern, P. Labeye, L. Lagny, F. Malbet, D. Malin, P. Maymoukov, S. Morel, C. Papaliolios, K. Perraut, M. Pearlman, I. L. Porro, I. Schanen, K. Souccar, G. Torres, and G. Wallace, “First Results with the IOTA3 Imaging Interferometer: The Spectroscopic Binaries λ Virginis and WR 140,” *ApJ***602**, L57–L60 (2004).
22. J. Berger, P. Haguenaue, P. Y. Kern, K. Rousselet-Perraut, F. Malbet, S. Gluck, L. Lagny, I. Schanen-Duport, E. Laurent, A. Delboulbe, E. Tatulli, W. A. Traub, N. Carleton, R. Millan-Gabet, J. D. Monnier, E. Pedretti, and S. Ragland, “An integrated-optics 3-way beam combiner for IOTA,” in *Interferometry for Optical Astronomy II. Edited by Wesley A. Traub . Proceedings of the SPIE, Volume 4838, pp. 1099-1106 (2003).*, pp. 1099–1106 (2003).
23. A. A. Michelson and F. G. Pease, “Measurement of the diameter of alpha Orionis with the interferometer.” *ApJ***53**, 249–259 (1921).
24. A. Labeyrie, “Interference fringes obtained on Vega with two optical telescopes,”

- ApJ**196**, L71–L75 (1975).
25. F. Vakili and L. Koechlin, “Aperture synthesis in space - Computer fringe blocking,” in *New technologies for astronomy; Proceedings of the Meeting, Paris, France, Apr. 25, 26, 1989 (A90-37976 16-89)*. Bellingham, WA, Society of Photo-Optical Instrumentation Engineers, 1989, p. 109-116., pp. 109–116 (1989).
 26. Y. Rabbia, S. Menardi, J. Gay, P. M. Boulton, P. Antonelli, M. Dugue, J. Marchal, F. Reynaud, M. Faucherre, and N. Hubin, “Prototype for the European Southern Observatory VLTI fringe sensor,” in *Proc. SPIE Vol. 2200, p. 204-215, Amplitude and Intensity Spatial Interferometry II, James B. Breckinridge; Ed.*, pp. 204–215 (1994).
 27. S. Robbe, B. Sorrente, F. Cassaing, Y. Rabbia, G. Rousset, L. Dame, P. Cruzalebes, and G. Schumacher, “Active phase stabilization at the I2T: implementation of the ASSI table,” in *Proc. SPIE Vol. 2200, p. 222-230, Amplitude and Intensity Spatial Interferometry II, James B. Breckinridge; Ed.*, pp. 222–230 (1994).
 28. P. R. Lawson, “Group-delay tracking in optical stellar interferometry with the fast Fourier transform,” *Optical Society of America Journal* **12**, 366–374 (1995).
 29. L. Koechlin, P. R. Lawson, D. Mourard, A. Blazit, D. Bonneau, F. Morand, P. Stee, I. Tallon-Bosc, and F. Vakili, “Dispersed fringe tracking with the multi- r_o apertures of the Grand Interferometre a 2 Telescopes,” *Appl. Opt.***35**, 3002–3009 (1996).
 30. P. Nisenson and W. Traub, “Magnitude Limit of the Group Delay Fringe Tracking Method for Long Baseline Interferometry,” in *Interferometric Imaging in Astronomy*, pp. 129–134 (1987).
 31. W. A. Traub and M. G. Lacasse, “Laboratory Measurements of Visibility Using Dispersed Fringes in Wavenumber Space,” in *NOAO-ESO Conference on High-Resolution Imaging by Interferometry: Ground-Based Interferometry at Visible and Infrared Wavelengths, Garching bei München, Germany, Mar. 15-18, 1988. Edited by F. Merkle, ESO Conference and Workshop Oroceedings No. 29, p.947, 1988*, pp. 947–954 (1988).
 32. W. A. Traub, “Constant-dispersion grism spectrometer for channeled spectra,” *Optical Society of America Journal* **7**, 1779–1791 (1990).
 33. W. A. Traub, M. G. Lacasse, and N. P. Carleton, “Spectral dispersion and fringe detection in IOTA,” in *Amplitude and intensity spatial interferometry; Proceedings of the Meeting, Tucson, AZ, Feb. 14-16, 1990 (A91-30676 12-89)*. Bellingham, WA, Society of Photo-Optical Instrumentation Engineers., pp. 145–152 (1990).
 34. D. F. Buscher, “Getting the most out of C.O.A.S.T.,” Ph.D. Thesis, University of Cambridge - Cavendish Laboratory (1988).
 35. K. T. Knox and B. J. Thompson, “Recovery of images from atmospherically degraded short-exposure photographs,” *ApJ***193**, L45–L48 (1974).
 36. F. Roddier, in *High-Resolution Imaging by Interferometry, ed. F. Merkle, ESO Conf.*

- Proc. 29 (Garching: ESO)*, pp. 565–571 (1988).
37. J. T. Armstrong, D. Mozurkewich, L. J. Rickard, D. J. Hutter, J. A. Benson, P. F. Bowers, N. M. Elias, C. A. Hummel, K. J. Johnston, D. F. Buscher, J. H. Clark, L. Ha, L.-C. Ling, N. M. White, and R. S. Simon, “The Navy Prototype Optical Interferometer,” *ApJ***496**, 550–571 (1998).
 38. P. R. Bevington and D. K. Robinson, *Data reduction and error analysis for the physical sciences* (New York: McGraw-Hill, —c1992, 2nd ed., 1992).